

# Identification and characterization of human UDP-glucuronosyltransferases responsible for the in-vitro glucuronidation of arctigenin

Hong Xin<sup>a\*</sup>, Yang-Liu Xia<sup>b\*</sup>, Jie Hou<sup>c</sup>, Ping Wang<sup>b</sup>, Wei He<sup>a</sup>, Ling Yang<sup>b</sup>, Guang-Bo Ge<sup>b</sup> and Wei Xu<sup>a</sup>

<sup>a</sup>Department of Integrated Traditional and Western Medicine, First Affiliated Hospital of Harbin Medical University, Harbin, <sup>b</sup>Laboratory of Pharmaceutical Resource Discovery, Dalian Institute of Chemical Physics, Chinese Academy of Sciences and <sup>c</sup>Department of Biochemistry and Molecular Biology, Dalian Medical University, Dalian, China

## Keywords

arctigenin; glucuronidation; human intestine microsomes; human liver microsomes; UDP-glucuronosyltransferases

## Correspondence

Guang-Bo Ge, Laboratory of Pharmaceutical Resource Discovery, Dalian Institute of Chemical Physics, Chinese Academy of Sciences, No. 457 Zhongshan Road, Dalian, 116023, China.

E-mail: geguangbo@dicp.ac.cn

Wei Xu, First Affiliated Hospital of Harbin Medical University, No. 23 Youzheng Street, Harbin, 150001, China.

E-mail: 13796059990@163.com

Received April 17, 2015

Accepted July 28, 2015

doi: 10.1111/jphp.12483

\*These authors contributed equally to this work.

## Abstract

**Objectives** This study aimed to characterize the glucuronidation pathway of arctigenin (AR) in human liver microsomes (HLM) and human intestine microsomes (HIM).

**Methods** HLM and HIM incubation systems were employed to catalyse the formation of AR glucuronide. The glucuronidation activity of commercially recombinant UGT isoforms towards AR was screened. A combination of chemical inhibition assay and kinetic analysis was used to determine the UGT isoforms involved in the glucuronidation of AR in HLM and HIM.

**Key findings** AR could be extensively metabolized to one mono-glucuronide in HLM and HIM. The mono-glucuronide was biosynthesized and characterized as 4'-O-glucuronide. UGT1A1, 1A3, 1A7, 1A8, 1A9, 1A10, 2B4, 2B7 and 2B17 participated in the formation of 4'-O-G, while UGT2B17 demonstrated the highest catalytic activity in this biotransformation. Both kinetic analysis and chemical inhibition assays demonstrated that UGT1A9, UGT2B7 and UGT2B17 played important roles in AR-4'-O-glucuronidation in HLM. Furthermore, HIM demonstrated moderate efficiency for AR-4'-O-glucuronidation, implying that AR may undergo a first-pass metabolism during the absorption process.

**Conclusion** UGT1A9, UGT2B7 and UGT2B17 were the major isoforms responsible for the 4'-O-glucuronidation of AR in HLM, while UGT2B7 and UGT2B17 were the major contributors to this biotransformation in HIM.

## Introduction

*Fructus Arctii* (Niubangzi), the dried fruits of *Arctium lappa* L. (also known as burdock) (Asteraceae), is one of the most popular traditional Chinese medicines. *Fructus Arctii* has been widely used for dispelling pathogenic wind-heat, promoting eruption, relieving sore throat, removing toxic substances and subduing swelling.<sup>[1]</sup> In China, a unique tea made from *Fructus Arctii* is commonly used as a health care product, which is useful for the treatment of tonsillitis, pharyngolaryngitis and constipation.<sup>[2]</sup> Arctigenin (AR, Figure 1) is one of the major lignin compounds in *Fructus Arctii*, with a high content of 9.7 mg/g of dry materials.<sup>[3]</sup> AR has been reported to exhibit anti-influenza,<sup>[4]</sup> anti-HIV,<sup>[5]</sup> anticancer through inducing cytotoxicity<sup>[6]</sup> and apoptosis,<sup>[7]</sup> antioxidative,<sup>[8]</sup> chemopreventive, anti-

inflammatory,<sup>[9]</sup> immunomodulative,<sup>[10]</sup> and anti-diabetic<sup>[11]</sup> activity. AR and its glucoside arctiin (AR-4'-O-β-glucoside) are phenylpropanoid dibenzylbutyrolactone lignans; they often coexist in several traditional Chinese herbals, such as *Arctium lappa* L., *Torreya nucifera* and *Saussurea medusa*, etc.<sup>[12]</sup> The amount of arctiin in these herbals is much higher than that of AR usually by an order of magnitude.<sup>[13]</sup> A previous study reported that arctiin (AR-4'-O-β-glucoside) could be extensively hydrolysed to AR by intestinal microflora, after oral administration of arctiin in rat.<sup>[12]</sup> This finding suggested that the aglycone rather than arctiin itself was the major constituent in circulating system after oral administration of arctiin-containing herbals; it also implied that the in-vivo pharmaceutical

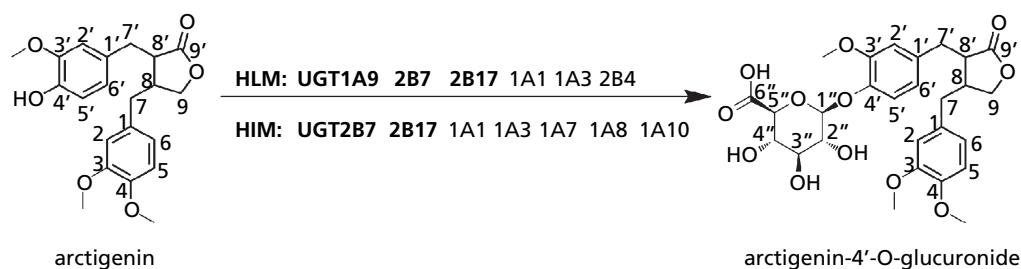


**Figure 1** Glucuronidation pathway of arctigenin.

effects of arctiin should be attributed to AR or its constitutive metabolite(s).

It was reported that AR could undergo both phase I and phase II metabolisms after administration in the rat; the biotransformations including hydrolysis, glucuronidation and demethylation lead to formations of arctigenic acid, AR-4'-O-glucuronide and 4-O-demethyl-AR, respectively.<sup>[12]</sup> It also has been revealed that arctigenic acid and AR-4'-O-glucuronide, rather than parent compound AR or 4-O-demethyl-AR, were the major compounds found in plasma after oral administration of AR in rats.<sup>[14]</sup> However, most of the previous studies concerning the glucuronidation process of AR were conducted in rat or in rat liver microsomes (RLM), and the glucuronidation pathway of AR in human tissues has not been reported yet. Therefore, it is necessary to characterize the glucuronidation pathway(s) of AR in human tissues.

It is well known that identification of major metabolites and the involved drug-metabolizing enzymes is very helpful for the elucidation of the metabolic and elimination pathways of a given drug or xenobiotic in human body, and for the deep understanding of its in-vivo effects. Therefore, this study aimed to characterize the glucuronidation pathway(s) of AR and to identify the human UGT isoform(s) responsible for the formation of the generated metabolite(s), by using recombinant human UGTs, human liver microsomes (HLM) and human intestine microsomes (HIM). In addition, the contributions of the major human UGTs in HLM and HIM, as well as the hepatic and intestinal clearance of AR via glucuronidation pathway, were also investigated.

## Materials and Methods

### Materials

AR, magnolol and nilotinib were purchased from Sichuan Victory Biotechnology Co. Ltd. (Sichuan, China). Alamethicin, Brij 58, magnesium chloride, D-saccharic acid 1,4-lactone,  $\beta$ -glucuronidase (EC No. 3.2.1.31), uridine-diphospho-glucuronic acid trisodium salt (UDPGA),

androsterone and testosterone were purchased from Sigma-Aldrich (St Louis, MO, USA). Pooled HLM from 11 donors (Lot. SUBK) and pooled SD rat liver microsomes from 100 donors (Lot. BDVH) were purchased from the Research Institute for Liver Diseases (Shanghai, China), and pooled HIM from 10 donors (Lot. UGU) was purchased from Celsis (Baltimore, MD, USA). A panel of recombinant human UGT isoforms (UGT1A1, -1A3, -1A4, -1A6, -1A7, -1A8, -1A9, -1A10, -2B4, -2B7, -2B15, and -2B17) expressed in baculovirus-infected insect cells were purchased from BD Gentest (Woburn, MA, USA). All other reagents were of HPLC grade or of the highest grade commercially available.

### Glucuronidation assay of arctigenin in human liver microsomes by LC-MS

The volumes of 200- $\mu$ l incubation mixture contained 50 mM Tris-HCl buffer (pH 7.4), 5 mM  $MgCl_2$ , 4 mM UDPGA, 25  $\mu$ g/ml alamethicin, 0.1 mg/ml HLM and 100  $\mu$ M AR. The reaction was initiated by the addition of UDPGA after pre-incubation at 37°C for 3 min. At 30-min incubation, the reaction was terminated with 200  $\mu$ l cold acetonitrile, followed by centrifugation at 20 000  $\times$  g for 20 min to obtain the supernatant for high-performance liquid chromatography spectrometry (HPLC) analysis. Control incubations without UDPGA or without substrate or without microsomes were performed to confirm that the metabolite produced were microsomes- and UDPGA-dependent.

Enzymatic hydrolysis was performed to confirm the glucuronide of AR. After incubation for 30 min in 200- $\mu$ l glucuronidation reaction mixture (without D-saccharic acid 1,4-lactone), an equal volume of 0.15 M acetate buffer (pH 5.0) with or without 1800 Fishman units of  $\beta$ -glucuronidase was added to the reaction mixture. After incubation for another 30 min at 37°C, the hydrolysis reaction was terminated by addition of 200- $\mu$ l cold acetonitrile, and then centrifuged at 20 000  $\times$  g for 20 min; the supernatant was injected to HPLC-UV analysis.

## Analytical instruments and conditions

AR and its glucuronide were analysed by an LC system (Shimadzu, Kyoto, Japan) containing an SCL-30A system controller, two LC-30AD pumps, a SIL-30AC auto-injector, a DGU-20AC vacuum degasser, a CTO-30AC column oven and a SPD-20AVP UV detector. A Shim-pack VP-ODS (5  $\mu\text{m}$ , 150.0 mm  $\times$  2.1 mm, Shimadzu) analytical column with an ODS guard column (2.2  $\mu\text{m}$ , 5.0 mm  $\times$  2.0 mm) was used to separate AR and its glucuronide. Column temperature was kept at 40°C. Acetonitrile (A) and water with 0.2% formic acid (B) as mobile phase at a flow rate of 0.4 ml/min, with a gradient of 0–9.0 min, 90% B–45% B; 9.0–12.0 min, 45% B; 12.0–15.0 min, balance to 90% B. The detection wavelength was set at 280 nm. Mass detection was performed on a Shimadzu LC-MS-2010EV instrument with an ESI interface both in positive and negative ion mode from  $m/z$  200 to 800. The detector voltage was set at +1.55 kV and 11.55 kV for positive and negative ion detection, respectively. The curved desolvation line temperature (CDL) and the block heater temperature were both set at 250°C, while the CDL voltage was set at 40V. Other MS detection conditions were set as follows: interface voltage, +4.5 kV and 14.0 kV for positive and negative ion detection, respectively; nebulizing gas ( $\text{N}_2$ ) flow, tuned to be 1.5 L/min; and the drying gas ( $\text{N}_2$ ) pressure 0.06 MPa. Data processing was performed using HPLC-MS Solution version 3.41 software (Shimadzu).

Quantification of AR glucuronidation in the incubation mixtures was accomplished by using the standard curve of the glucuronide, which has a linear range from 0.1 to 10  $\mu\text{M}$  (the correlation coefficient was 0.999). The accuracy and precision of the intra-day and inter-day error were both less than 3%.

## Biosynthesis of glucuronide and structural characterization

The metabolite of AR was biosynthesized using RLM and purified for structure elucidation and quantitative analysis. In brief, 1 mM AR was incubated with RLM (0.5 mg protein/ml), 0.1 M Tris-HCl (pH 7.4), 10 mM  $\text{MgCl}_2$ , Brij 58 (0.5 mg/mg protein), 10 mM D-saccharic acid 1,4-lactone, and 4 mM UDPGA in 20 ml of final incubations for 12 h at 37°C. The stock solution of AR (100 mM) was prepared in DMSO. The concentration of organic solvent in the final incubation was 1%. The reaction was terminated by adding 20 ml acetonitrile and then transferred the vessel to an ice bath and cooled for 20 min. After removal of protein by centrifugation at 20 000  $\times$  g for 30 min at 4°C, the combined supernatants were loaded on an SPE cartridge (C18, 1000 mg, Agela Technologies, Radnor, PA, USA), which was preconditioned by sequential washing with 6-ml methanol and 6-ml Millipore water. After sample

loading, the SPE cartridge was sequentially eluted with 12-ml Millipore water, 12-ml methanol and 12-ml methanol containing 5% formic acid. The entire process was monitored by HPLC, and the metabolite was assembled in methanol containing 5% formic acid. After vacuum evaporation, the residue was re-dissolved in 1-ml methanol and separated by HPLC. The purity was greater than 95% according to HPLC-UV analysis. The structure of metabolite was determined by nuclear magnetic resonance (NMR), and the experiment contained a Varian INOVA-500 NMR spectrometer (Varian, Palo Alto, CA, USA). The purified 5.4-mg metabolites were stored at –20°C before dissolving in dimethyl sulfoxide- $d_6$  (Euriso-Top, Saint-Aubin, France) for NMR analysis. Chemical shifts were given on  $\delta$  scale and referenced to tetramethylsilane at 0 ppm for  $^1\text{H}$ -NMR (500 MHz) and  $^{13}\text{C}$ -NMR (100 MHz).

## Assay with recombinant UGTs

AR glucuronidation was measured in reaction mixtures containing recombinant human UGT1A1, 1A3, 1A4, 1A6, 1A7, 1A8, 1A9, 1A10, 2B4, 2B7, 2B15 and 2B17. The incubations were conducted as described above for the HLM study, in the presence of 100  $\mu\text{M}$  substrate. The final protein concentration of the reactions was 0.1 mg/ml and incubated at 37°C for 60 min. Liquid chromatography with ultraviolet (LC-UV) and liquid chromatography-electrospray ionization-mass spectrometry (LC-ESI-MS) detection was used to monitor the metabolite.

## Chemical inhibition assays

Glucuronidation of AR in pooled HLM and HIM was measured in the absence or presence of an inhibitor (nilotinib, magnolol, androsterone or testosterone). Nilotinib is a selective inhibitor of UGT1A1.<sup>[15]</sup> Magnolol is an effective inhibitor for UGT1A9,<sup>[16]</sup> and androsterone is reported to be able to inhibit both UGT1A9 and UGT2B7.<sup>[17]</sup> Testosterone is a specific substrate of UGT2B17 with the  $K_m$  value of 10  $\mu\text{M}$ .<sup>[18]</sup> AR (15  $\mu\text{M}$  in HLM and 25  $\mu\text{M}$  in HIM) was incubated in the absence or presence of nilotinib (10  $\mu\text{M}$ ), magnolol (1  $\mu\text{M}$ ) androsterone (10  $\mu\text{M}$ ) or testosterone (25  $\mu\text{M}$ ). The incubations were performed for 15 min at a protein concentration of 0.01 mg/ml in HLM or of 0.05 mg/ml in HIM.

## Kinetic characterization

The formation rate of AR glucuronide was linear over 20 min of incubation and 0.01–0.1 mg of microsomal protein. To ensure that less than 10% of substrate was metabolized in all incubations, the kinetic determinations were carried out using a microsomal protein concentration of 0.01 mg/ml (HLM) and 0.05 mg/ml (HIM) with 15-min

incubation. To estimate kinetic parameters, AR (1–200  $\mu\text{M}$ ) was incubated with pooled HLM and HIM. For recombinant human UGTs, AR (1–200  $\mu\text{M}$ ) was incubated with each isoenzyme for 15 min; the final protein concentration was 0.1 mg/ml for UGT1A1 and UGT1A7, 0.02 mg/ml for UGT1A9, 0.05 mg/ml for UGT2B7, and 0.025 mg/ml for UGT2B17. Kinetic parameters for AR glucuronidation in HLM, HIM and UGTs were obtained by fitting the Michaelis–Menten equation to experimental data using GraphPad Prism 6.0 (GraphPad Software, San Diego, CA, USA). The Michaelis–Menten equation is  $v = V_{\text{max}}[S]/(K_m + [S])$ , where  $v$  is the rate of reaction,  $V_{\text{max}}$  is the maximum velocity,  $K_m$  is the Michaelis constant (substrate concentration at 0.5  $V_{\text{max}}$ ), and  $[S]$  is the substrate concentration. Results were expressed as mean  $\pm$  S.E. of triplicate independent determinations.

### Statistical analysis

Data from chemical inhibition studies are expressed as means and SDs. Statistical analyses are performed with one-way analysis of variance. Differences were considered statistically significant when  $P < 0.05$ .

## Results

### Identification of arctigenin glucuronide

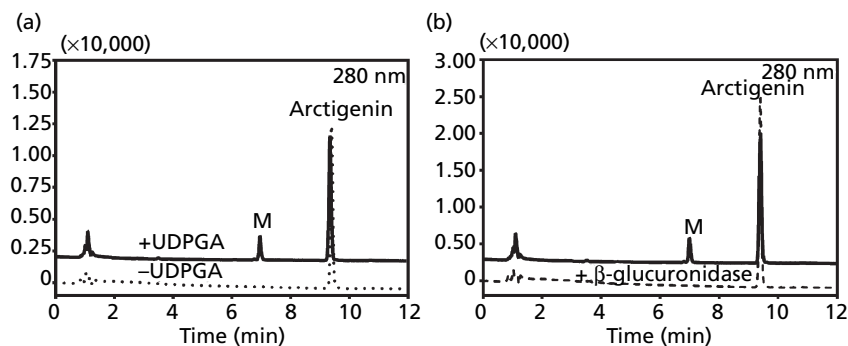
After incubation with AR (100  $\mu\text{M}$ ) and HLM (0.1 mg/ml) in the presence of UDPGA, the metabolite was identified by HPLC-ESI-MS, and the retention time of the one new peak was 6.9 min (Figure 2a). The peak was not detected in the control incubations without UDPGA, AR or microsomes. The negative ion mode was adopted for identification AR and its glucuronide, as it is more sensitive than the positive ion mode for these two compounds. The mass spectra was dominated by  $[\text{M}-\text{H}]^-$  ion at  $m/z$  547.4, corresponding to the mono-glucuronide of AR with characteristic  $m/z$  176. In

addition, AR glucuronide can be rapidly hydrolysed by  $\beta$ -glucuronidase to the parent AR (Figure 2b), further proving that it is the mono-glucuronide metabolite.

Then the metabolite was biosynthesized by using RLM, and then its chemical structure was well characterized by  $^1\text{H-NMR}$  and  $^{13}\text{C-NMR}$ . The  $^1\text{H-NMR}$  and  $^{13}\text{C-NMR}$  spectral data of the metabolite were listed in Table 1. Compared with NMR data of AR, the  $^{13}\text{C-NMR}$  spectrum of the glucuronide displayed the carbon signal of C-4' ( $\delta$ ) shifted upfield to  $\delta 144.75$  ( $\Delta\delta -0.32$ ), which is probably due to a glycosidation shift of a phenolic compound. In the sugar moiety, the G1 protons and carbons exhibited characteristic chemical shifts near 5 and 100 ppm, whereas the G6 carbon ( $-\text{COOH}$ ) showed chemical shifts of approximately 170 ppm. In addition, the  $\beta$ -configuration of the glucuronic acid moiety was confirmed by the coupling constant of the anomeric proton ( $\delta 5.01$ ,  $J = 7.0$  Hz), which agreed well with previous reports regarding the O-glucuronides.<sup>[19]</sup> All these evidence clearly demonstrated that the glucuronidation site was located at the C-4' phenolic group of AR and the glucuronide was identified as AR-4'-O-glucuronide (Figure 1).

### Assay with recombinant human UGTs

Twelve recombinant UGTs, namely UGT1A1, 1A3, 1A4, 1A6, 1A7, 1A8, 1A9, 1A10, 2B4, 2B7, 2B15 and 2B17, were used to catalyse AR glucuronidation and determine the pivotal isoforms responsible for the metabolism pathway. With the substrate concentration of 100  $\mu\text{M}$ , UGT1A1, UGT1A3, UGT1A7, UGT1A9, UGT1A10, UGT2B4, UGT2B7 and UGT2B17 participated in the formation of AR-4'-O-glucuronide (Figure 3). Compared with other isoforms, UGT2B17 displayed a relative higher activity to the formation of AR-4'-O-glucuronide, followed by UGT1A9, UGT1A1 and UGT2B7, while UGT1A3, UGT1A8 and UGT1A10 demonstrated relative low efficiency in the glucuronidation of AR.

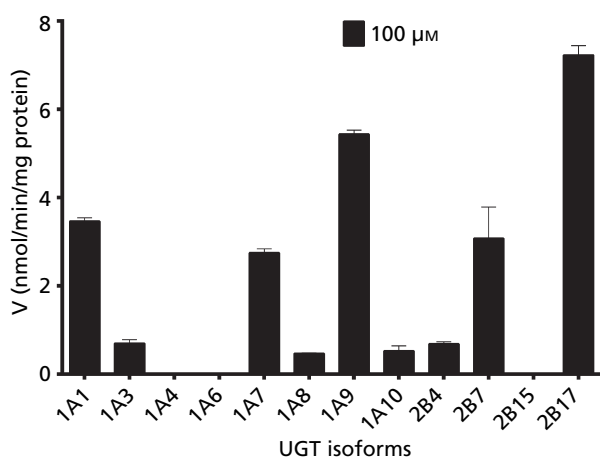
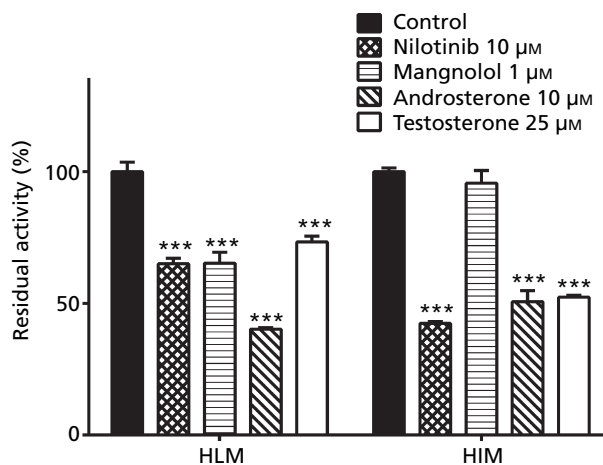


**Figure 2** Representative LC-UV profile of arctigenin and its glucuronide in human liver microsomes. (a) Arctigenin was incubated in human liver microsomes with (solid line) and without (dotted line) UDPGA for 30 min. (b) Arctigenin was incubated in human liver microsomes without (solid line) and with (dashed line)  $\beta$ -glucuronidase for 30 min.

**Table 1**  $^1\text{H-NMR}$  and  $^{13}\text{C-NMR}$  data for AR and its glucuronide

Position	AR		AR-O-glucuronide	
	$\delta^1\text{HMult}$ ( $J$ in Hz)	$\delta^{13}\text{C}$	$\delta^1\text{HMult}$ ( $J$ in Hz)	$\delta^{13}\text{C}$
1	–	128.83	–	131.13
2	6.59 d (4.6)	113.44	6.58 d (8.0)	113.91
3	–	147.36	–	148.64
4	–	147.29	–	147.29
5	6.74	111.87	6.78	111.89
6	6.60 d (1.8)	120.33	6.58 d (8.0)	120.37
7	2.50	36.83	2.71	36.85
8	2.68	40.74	2.72	40.70
9	4.07	70.61	4.12	71.36
1'	–	131.21	–	132.18
2'	6.68 d(8.0)	112.41	6.67 d (7.9)	112.41
3'	–	148.64	–	148.78
4'	–	145.07	–	144.75
5'	6.82 d(8.1)	115.25	6.82 d (8.1)	115.16
6'	6.63 d(1.8)	121.51	6.59 d (8.0)	121.22
7'	2.84 d (5.3)	33.67	3.05 d (7.0)	33.55
8'	2.74	45.60	2.74	45.51
9'	–	178.36	–	178.32
CH <sub>3</sub> O	3.70 (3H, s)	55.32	3.81 (3H, s)	55.36
CH <sub>3</sub> O	3.70 (3H, s)	55.44	3.83 (3H, s)	55.45
CH <sub>3</sub> O	3.70 (3H, s)	55.51	3.86 (3H, s)	55.59
G1	–	–	5.01 d (7.0)	99.88
G2	–	–	3.37 m	72.93
G3	–	–	3.31 m	75.75
G4	–	–	3.39 m	71.36
G5	–	–	3.69 m	76.01
G6	–	–	–	169.18

AR, arctigenin.

**Figure 3** The formation of AR-4'-O-glucuronide catalysed by various recombinant human UGTs. Arctigenin (100  $\mu\text{M}$ ) was incubated with various recombinant human UGTs (0.1 mg/ml) at 37°C for 60 min. Data represent the mean of triplicate incubations.**Figure 4** Inhibitory effects of nilotinib, maganolol, androsterone and testosterone on the formation of arctigenin glucuronidated metabolite in human liver microsomes and human intestine microsomes. Arctigenin (15  $\mu\text{M}$  in human liver microsomes and 25  $\mu\text{M}$  in human intestine microsomes) was incubated with human liver microsomes (0.01 mg of protein/ml) or human intestine microsomes (0.05 mg of protein/ml) with either nilotinib (10  $\mu\text{M}$ ), maganolol (1  $\mu\text{M}$ ), androsterone (10  $\mu\text{M}$ ) or testosterone (25  $\mu\text{M}$ ) at 37°C for 15 min. \*\*\* $P < 0.001$  compared with control. Data represent the mean  $\pm$  SD ( $n = 3$ ).

### Chemical inhibition assays

To reveal the importance of UGT1A1, UGT1A9, UGT2B7 and UGT2B17 in the formation of AR-4'-O-glucuronide in HLM and in HIM, a series of inhibition assays were elucidated by using selective inhibitors. As shown in Figure 4, magnanolol and testosterone exhibited similar inhibitory effects on AR-4'-O-glucuronidation. The residual activity of HLM was 65% and 73% for the formation of AR-4'-O-glucuronide in the presence of magnanolol and testosterone, respectively, indicating that the contribution of UGT1A9 or UGT2B17 in the formation of the glucuronide was about 30%, respectively. For the formation of AR-4'-O-glucuronide, the remaining activity of HLM was less than 40% in the presence of androsterone, indicating that UGT2B7 also played an important role in AR-4'-O-glucuronidation. Furthermore, upon addition of nilotinib, which could inhibit both UGT1A1 and UGT2B17 (data not show), the formation of AR-4'-O-glucuronide in HLM could be inhibited by about 40% of control, implying that the contribution of UGT1A1 for AR-4'-O-glucuronidation was about 10%. The similar inhibition assays were also conducted in HIM, as shown in Figure 4; androsterone or testosterone could inhibit the formation of AR-4'-O-glucuronide in HIM significantly with the residual activity of 50%, while the formation of AR-4'-O-glucuronide in HIM could be inhibited near 60% by addition of nilotinib.

**Table 2** Kinetic parameters of arctigenin AR glucuronidation in human liver microsomes, human intestine microsomes and recombinant UGTs

Enzyme Source	$V_{max}$ (nmol/min/mg)	$K_m$ ( $\mu$ M)	$V_{max}/K_m$ ( $\mu$ l/min/mg)
HLM	67.0 $\pm$ 1.0	15.8 $\pm$ 1.0	4240
HIM	19.1 $\pm$ 0.3	24.6 $\pm$ 1.3	776
UGT1A1	0.69 $\pm$ 0.01	6.0 $\pm$ 0.7	114
UGT1A7	2.3 $\pm$ 0.08	61.1 $\pm$ 5.4	37
UGT1A9	6.5 $\pm$ 0.2	19.1 $\pm$ 1.7	342
UGT2B7	2.8 $\pm$ 0.07	5.2 $\pm$ 0.6	548
UGT2B17	12.0 $\pm$ 0.3	5.4 $\pm$ 0.5	2207

AR, arctigenin; HIM, human intestine microsomes; HLM, human liver microsomes.

These findings suggested that UGT2B7 and UGT2B17 were two major contributors in the formation of AR-4'-O-glucuronide in HIM, and the contribution of UGT1A1 for AR-4'-O-glucuronidation in HIM was about 10%. In sharp contrast, magnolol had no effects on the formation of AR-4'-O-glucuronide in HIM, suggesting that UGT1A9 did not participate in intestinal glucuronidation of AR.

### Kinetic characterization

The kinetic parameters including  $K_m$ ,  $V_{max}$  and the intrinsic clearance ( $V_{max}/K_m$ ) for AR-4'-O-glucuronidation in HLM, HIM and the potent UGT isoforms were determined and shown in Table 2. The range of substrate concentrations was from 1 to 200  $\mu$ M for the kinetic analyses. In the concentration range tested, AR-4'-O-glucuronidation in HLM, HIM and in human UGTs isoforms, including UGT1A1, UGT1A7, UGT1A9, UGT2B7 and UGT2B17, exhibited Michaelis–Menten kinetics, as evidenced by a linear Eadie–Hofstee plot (Figure 5). The kinetic parameters of AR-4'-O-glucuronidation in UGT1A3, UGT1A8, UGT1A10 and UGT2B4 could not be characterized as the formation rates of AR glucuronide in these isoforms were very slow. The  $K_m$  values for the formation of the metabolite in HLM and HIM were 15.8  $\mu$ M and 24.6  $\mu$ M; the  $V_{max}$  values were 67.0 and 19.1 nmol/min/mg protein; and the clearance values were determined to be 4240 and 776  $\mu$ l/min/mg protein, respectively. In recombinant UGT1A1, UGT1A7, UGT1A9, UGT2B7 and UGT2B17, the  $K_m$  values were 6.0, 61.1, 19.1, 5.2 and 5.4  $\mu$ M, respectively; the  $V_{max}$  values were 0.69, 2.3, 6.5, 2.8 and 12.0 nmol/min/mg protein, respectively; and the clearance values were calculated to be 114, 37, 342, 548 and 2207  $\mu$ l/min/mg protein, respectively.

### Discussion

As a major bioactive compound in several traditional Chinese herbs, AR has drawn much attention in the past

20 years. Modern pharmacological studies around the world have clearly shown that AR possesses diverse pharmacological activity, including anti-influenza, anti-oxidation and immunomodulation, and most of these activities are beneficial to human health.<sup>[20]</sup> In contrast to the extensive studies on the pharmacological activity, the metabolic pathways and metabolic behaviours of AR in human and experimental animals have not been well investigated. More recently, a metabolic profiling study revealed that AR could be metabolized to several phase I and phase II metabolites after oral administration in rat, while glucuronidation was one of the major metabolic pathways in rat.<sup>[12]</sup> Our preliminary study on in-vitro metabolism of AR also found that AR could be rapidly glucuronidated in HLM, while the formation of phase I metabolites in HLM was very slow. This finding inspired us to characterize the glucuronidation pathway(s) of AR in human tissues.

Our results demonstrated that AR could be rapidly glucuronidated in both HLM and HIM in the presence of UGPA, while a mono-glucuronide was formed. The glucuronide was biosynthesized and then fully characterized as AR-4'-O-glucuronide. Reaction phenotyping by using commercially available UGT enzymes demonstrated that at least six UGT1A isoforms participated in AR-4'-O-glucuronidation, while three UGT2B isoforms, namely UGT2B4, UGT2B7 and UGT2B17, could catalyse this biotransformation. Notably, three most abundantly expressed UGT isoforms in human liver, namely UGT1A9, UGT2B7 and UGT2B17, are major contributors to AR-4'-O-glucuronidation in human liver, which is confirmed by the chemical inhibition assays. Given the abundant expression of these three major UGT isoforms in human liver and the good catalytic efficiency of these enzymes, the high intrinsic clearance of AR-4'-O-glucuronidation in HLM (4241  $\mu$ l/min/mg protein) is not so surprising.

It is also worthy to mention that the corresponding  $Cl_{int}$  of AR in RLM was 129  $\mu$ l/min/mg according to a previous report,<sup>[21]</sup> which is much lower than that in HLM as demonstrated in this study. This could be partially explained by the fact that rat UGT1A9 is a pseudogene and the propofol O-glucuronidation activity in rat liver is much lower than that in human liver.<sup>[22,23]</sup> These findings agreed well with the observation of rapid formation of 4'-O-glucuronide after both oral and IV administration of AR,<sup>[21]</sup> indicating that AR may be rapidly eliminated from human body via glucuronidation pathway.

The formation of AR-4'-O-glucuronidation could also be observed in HIM, which is consistent with previous report that AR could be transformed to its 4'-O-glucuronide in rat intestine microsomes.<sup>[21]</sup> The kinetic analysis demonstrated that human intestine played an important role in AR-4'-O-glucuronidation with  $Cl_{int}$  value of 776  $\mu$ l/min/mg protein in HIM, implying that AR may undergo a first-pass

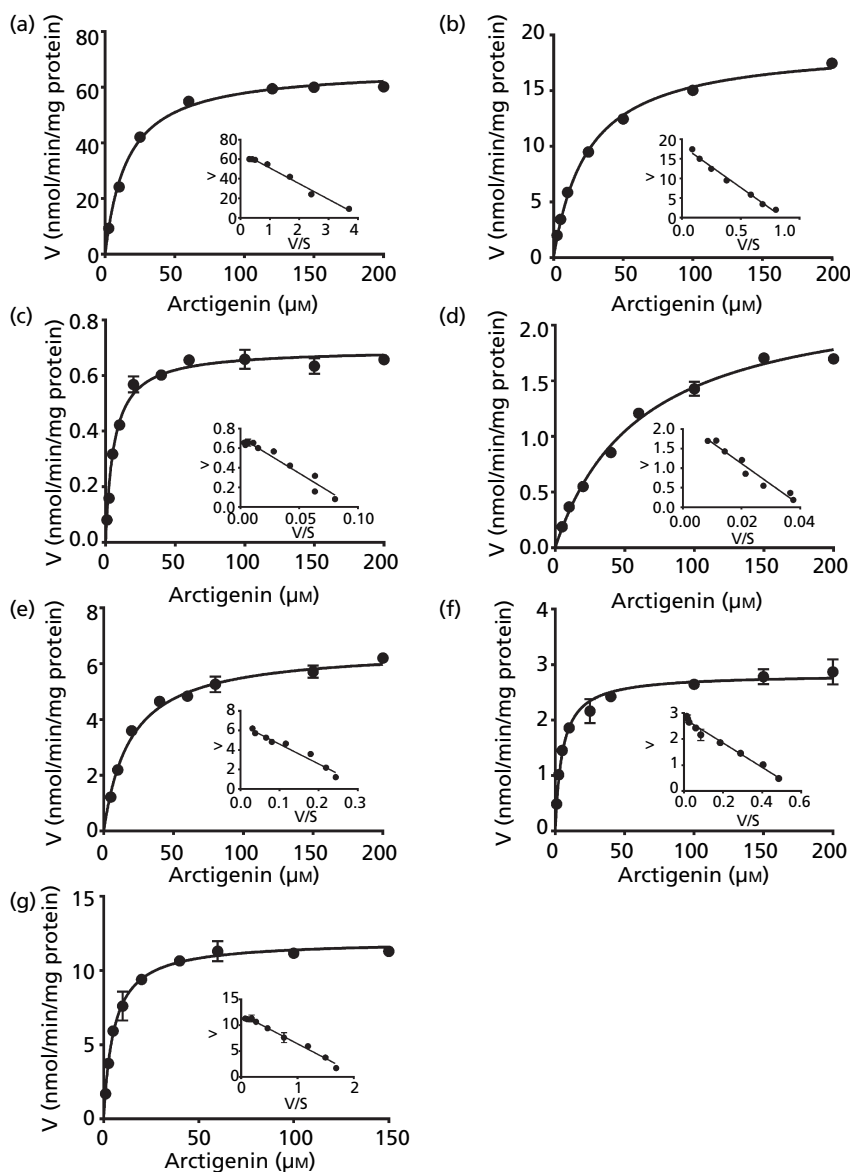


**Figure 5** Enzyme kinetics of AR-4'-O-glucuronidation by human liver microsomes (a), human intestine microsomes (b), UGT1A1 (c), UGT1A7 (d), UGT1A9 (e), UGT2B7 (f) and UGT2B17 (g). Arctigenin (1–200  $\mu\text{M}$ ) was incubated with pooled human liver microsomes (0.01 mg of protein/ml), human intestine microsomes (0.05 mg of protein/ml), UGT1A1 (0.1 mg of protein/ml), UGT1A7 (0.1 mg of protein/ml), UGT1A9 (0.02 mg of protein/ml), UGT2B7 (0.05 mg of protein/ml) and UGT2B17 (0.025 mg of protein/ml) at 37°C for 15 min. An Eadie–Hofstee plot was shown as an inset to illustrate monophasic kinetics.

metabolism during the absorption process. Actually, an extensive first-pass metabolism of AR to arctigenin-4'-O-glucuronide was also observed in an intestinal perfusion study in rat, with Cummins's extraction ratio of  $0.085 \pm 0.013$ .<sup>[14]</sup>

Apart from the rapid glucuronidation of AR in human liver and intestine, kidney may also participate in AR-4'-O-glucuronidation in human body. Taking into account the fact that UGT1A9 demonstrated a high catalytic activity towards AR-4'-O-glucuronidation and its abundant expres-

sion in kidney,<sup>[24]</sup> UGT1A9 may be the major contributor to the metabolic clearance of AR in human kidney. Considering that UGT1A9 and UGT2B7 are highly expressed in these metabolic organs of human,<sup>[25]</sup> as well as the high catalytic activity of these UGT isoforms in AR-4'-O-glucuronidation, it is readily conceivable that AR could be extensively glucuronidated after oral administration in human body. Therefore, the activity of AR-4'-O-glucuronide and the excretion of this glucuronide should be further investigated.

Furthermore, among the major isoforms participated in AR-4'-O-glucuronide, UGT2B17 is one of the major contributors in both human liver and intestine, leading to a rapid metabolic elimination of AR from human body. It has been reported that the individuals possessing mutant UGT2B17 (UGT2B17\*2) exhibit the absence of UGT2B17 protein.<sup>[26]</sup> The UGT2B17\*2/\*2 genotype is strongly associated with low activity towards testosterone, a selective substrate of UGT2B17.<sup>[27]</sup> The frequency of the UGT2B17\*2/\*2 genotype was reported to be 67% and >80% in Korean<sup>[28]</sup> population and Japanese population,<sup>[29]</sup> respectively, indicating that UGT2B17 protein may be absent in many Asian people. It is easily conceivable that a prolongation of the residence time and an increased exposure of AR may be frequently observed in Asian people or other individuals possessing UGT2B17\*2/\*2. The in-vivo decreased efficiency of UGT2B17-mediated AR-4'-O-glucuronidation in the individuals possessing UGT2B17\*2/\*2 should be further investigated.

Despite of UGT2B17, UGT1A1 and UGT2B7 also play important roles in the hepatic and intestinal glucuronidation of AR. It has been reported that many therapeutic drugs, natural bioactive compounds and herbal medicines could potentially inhibit UGT1A1 and UGT2B7, such as an immunosuppressant drug tacrolimus,<sup>[30]</sup> a natural flavonoid silybin,<sup>[31]</sup> and a ginsenoside20(S)-protopanaxatriol,<sup>[32]</sup> as well as *Andrographis paniculata* extracts.<sup>[33]</sup> Co-administration with these drugs or herbs could be helpful for prolongation of the residence time and increasing the exposure of AR in human body, via inhibiting UGT1A1- and UGT2B7-mediated AR-4'-O-glucuronidation.

Taken together, AR could be extensively metabolized by human UGTs and generates one mono-glucuronides (4'-O-glucuronide). Both kinetic characterization and inhibition

assays demonstrated that UGT1A9, UGT2B7 and UGT2B17 played important roles in hepatic glucuronidation of AR, while UGT2B7 and UGT2B17 were two major contributors to the formation of AR-4'-O-glucuronide in HIM. In addition, the  $Cl_{int}$  of 4'-O-glucuronide of AR generated in HIM indicated a first-pass metabolism in the intestinal border after oral administration, and the following hepatic glucuronidation should lead to a rapid elimination of arctigenin from human body.

## Conclusions

In conclusion, the glucuronidation pathway of AR in HLM and HIM was well characterized for the first time. UGT1A9, UGT2B7 and UGT2B17 were the major isoforms responsible for the 4'-O-glucuronidation of AR in HLM, while UGT2B7 and UGT2B17 were the major contributors to this biotransformation in HIM.

## Declarations

### Conflict of interest

The Author(s) declare(s) that they have no conflicts of interest to disclose.

### Funding

This work was supported by the National S&T Major Projects of China (2012ZX09501001, 2012ZX09506001), the National Basic Research Program of China (2013CB531800), NSF of China (81473181, 81273590, 81302793), and the Leading Talent Research Fund of Harbin (2011RFXYS079).

## References

- Zhao F *et al.* In vitro anti-inflammatory effects of arctigenin, a lignan from *Arctium lappa* L., through inhibition on iNOS pathway. *J Ethnopharmacol* 2009; 122: 457–462.
- Yang YN *et al.* Hepatoprotective activity of twelve novel 7'-hydroxy lignan glycosides from *Arctii Fructus*. *J Agric Food Chem* 2014; 62: 9095–9102.
- Kravtsova SS, Khasanov VV. Lignans and fatty acid composition of *Arctium lappa* seeds. *Chem Nat Comp* 2011; 47: 800–801.
- Hayashi K *et al.* Therapeutic effect of arctiin and arctigenin in immunocompetent and immunocompromised mice infected with influenza A virus. *Biol Pharm Bull* 2010; 33: 1199–1205.
- Schroder HC *et al.* Differential in vitro anti-HIV activity of natural lignans. *Z Naturforsch C* 1990; 45: 1215–1221.
- Awale S *et al.* Identification of arctigenin as an antitumor agent having the ability to eliminate the tolerance of cancer cells to nutrient starvation. *Cancer Res* 2006; 66: 1751–1757.
- Wang L *et al.* Induction of apoptosis of the human leukemia cells by arctigenin and its mechanism of action. *Yao Xue Xue Bao* 2008; 43: 542–547.
- Shoeb M *et al.* Isolation, structure elucidation and bioactivity of schischkiniin, a unique indole alkaloid from the seeds of *Centaurea schischkinii*. *Tetrahedron* 2005; 61: 9001–9006.
- Kang K *et al.* The chemopreventive effects of *Saussurea salicifolia* through induction of apoptosis and phase II detoxification enzyme. *Biol Pharm Bull* 2007; 30: 2352–2359.
- Cho MK *et al.* Arctigenin, a phenylpropanoid dibenzylbutyrolactone lignan, inhibits MAP kinases and AP-1 activation via potent MKK inhibition: the role in TNF- $\alpha$  inhibition. *Int*

- Immunopharmacol* 2004; 4: 1419–1429.
11. Xu ZH *et al.* The antidiabetic activity of total lignan from *Fructus arctii* against alloxan-induced diabetes in mice and rats. *Phytother Res* 2008; 22: 97–101.
  12. Gao Q *et al.* Hydrolysis is the dominating in vivo metabolism pathway for arctigenin: identification of novel metabolites of arctigenin by LC/MS/MS after oral administration in rats. *Planta Med* 2013; 79: 471–479.
  13. Zhou XY *et al.* Determination of arctiin and arctigenin contents in *Arctium tomentosum* Mill. by HPLC method. *J Chem* 2011; 8: 372–376.
  14. Gao Q *et al.* Extensive intestinal first-pass metabolism of arctigenin: evidenced by simultaneous monitoring of both parent drug and its major metabolites. *J Pharm Biomed Anal* 2014; 91: 60–67.
  15. Fujita K *et al.* The small-molecule tyrosine kinase inhibitor nilotinib is a potent noncompetitive inhibitor of the SN-38 glucuronidation by human UGT1A1. *Cancer Chemother Pharmacol* 2011; 67: 237–241.
  16. Zhu LL *et al.* Potent and selective inhibition of magnolol on catalytic activities of UGT1A7 and 1A9. *Xenobiotica* 2012; 42: 1001–1008.
  17. Uchaipichat V *et al.* Selectivity of substrate (trifluoperazine) and inhibitor (amitriptyline, androsterone, canrenoic acid, hecogenin, phenylbutazone, quinidine, quinine, and sulfapyrazone) 'probes' for human UDP-glucuronosyltransferases. *Drug Metab Dispos* 2006; 34: 449–456.
  18. Sten T *et al.* UDP-glucuronosyltransferases (UGTs) 2B7 and UGT2B17 display converse specificity in testosterone and epitestosterone glucuronidation, whereas UGT2A1 conjugates both androgens similarly. *Drug Metab Dispos* 2009; 37: 417–423.
  19. Xia YL *et al.* Identification and characterization of human UDP-glucuronosyltransferases responsible for the glucuronidation of fraxetin. *Drug Metab Pharmacokinet* 2014; 29: 135–140.
  20. Chan YS *et al.* A review of the pharmacological effects of *Arctium lappa* (burdock). *Inflammopharmacology* 2011; 19: 245–254.
  21. Gao Q *et al.* Elucidation of arctigenin pharmacokinetics after intravenous and oral administrations in rats: integration of in vitro and in vivo findings via semi-mechanistic pharmacokinetic modeling. *AAPS J* 2014; 16: 1321–1333.
  22. Shiratani H *et al.* Species differences in UDP-glucuronosyltransferase activities in mice and rats. *Drug Metab Dispos* 2008; 36: 1745–1752.
  23. Liang SC *et al.* Determination of propofol UDP-glucuronosyltransferase (UGT) activities in hepatic microsomes from different species by UFLC-ESI-MS. *J Pharm Biomed Anal* 2011; 54: 236–241.
  24. Knights KM *et al.* Renal drug metabolism in humans: the potential for drug-endobiotic interactions involving cytochrome P450 (CYP) and UDP-glucuronosyltransferase (UGT). *Br J Clin Pharmacol* 2013; 76: 587–602.
  25. Sato Y *et al.* Optimized methods for targeted peptide-based quantification of human uridine 5'-diphosphate-glucuronosyltransferases in biological specimens using liquid chromatography-tandem mass spectrometry. *Drug Metab Dispos* 2014; 42: 885–889.
  26. Wilson W 3rd *et al.* Characterization of a common deletion polymorphism of the UGT2B17 gene linked to UGT2B15. *Genomics* 2004; 84: 707–714.
  27. Schulze JJ *et al.* Doping test results dependent on genotype of uridine diphospho-glucuronosyl transferase 2B17, the major enzyme for testosterone glucuronidation. *J Clin Endocrinol Metab* 2008; 93: 2500–2506.
  28. Jakobsson J *et al.* Large differences in testosterone excretion in Korean and Swedish men are strongly associated with a UDP-glucuronosyl transferase 2B17 polymorphism. *J Clin Endocrinol Metab* 2006; 91: 687–693.
  29. Terakura S *et al.* A UGT2B17-positive donor is a risk factor for higher transplant-related mortality and lower survival after bone marrow transplantation. *Br J Haematol* 2005; 129: 221–228.
  30. Liu XY *et al.* Tacrolimus strongly inhibits multiple human UDP-glucuronosyltransferase (UGT) isoforms. *Pharmazie* 2012; 67: 804–808.
  31. Jancova P *et al.* Evidence for differences in regioselective and stereoselective glucuronidation of silybin diastereomers from milk thistle (*Silybum marianum*) by human UDP-glucuronosyltransferases. *Xenobiotica* 2011; 41: 743–751.
  32. He YJ *et al.* The inhibitory effect of 20(S)-protopanaxatriol (ppt) towards UGT1A1 and UGT2B7. *Phytother Res* 2013; 27: 628–632.
  33. Ismail S *et al.* Effects of *Andrographis paniculata* and *Orthosiphon stamineus* extracts on the glucuronidation of 4-methylumbelliferone in human UGT isoforms. *Molecules* 2010; 15: 3578–3592.